TRANSPORTATION POOLED FUND PROGRAM
QUARTERLY PROGRESS REPORT

Lead Agency (FHWA or State DOT): ____Kansas DOT_____

INSTRUCTIONS:

Project Managers and/or research project investigators should complete a quarterly progress report for each calendar quarter during which the projects are active. Please provide a project schedule status of the research activities tied to each task that is defined in the proposal; a percentage completion of each task; a concise discussion (2 or 3 sentences) of the current status, including accomplishments and problems encountered, if any. List all tasks, even if no work was done during this period.

Transportation Pooled Fund Program Project # **TPF-5(328)**	**Transportation Pooled Fund Program - Report Period:** ☐Quarter 1 (January 1 – March 31) ☒Quarter 2 (April 1 – June 30) ☐Quarter 3 (July 1 – September 30) ☐Quarter 4 (October 1 – December 31)
Project Title: Strain-based Fatigue Crack Monitoring of Steel Bridges using Wireless Elastomeric Skin Sensors	
Project Manager: **Susan Barker, P.E.** **Phone:** **(785) 291-3847** **E-mail: SusanB@ksdot.org**	
Project Investigator: **Li Jian** **Phone:** **785-864-6850** **E-mail:** **jianli@ku.edu**	

Lead Agency Project ID: **RE-0699-01**	**Other Project ID (i.e., contract #):**	**Project Start Date:** **9/2015**
Original Project End Date: **Multi-year project**	**Current Project End Date:** **8/31/2018**	**Number of Extensions:** **N.A.**

Project schedule status:

☒ On schedule ☐ On revised schedule ☐ Ahead of schedule ☐ Behind schedule

Overall Project Statistics:

Total Project Budget	Total Cost to Date for Project	Total Percentage of Work Completed
$405,000	**$ 66,788.52**	**25%**

Quarterly Project Statistics:

Total Project Expenses This Quarter	Total Amount of Funds Expended This Quarter	Percentage of Work Completed This Quarter
$ 51,089.21	**$ 51,089.21**	**10%**

Project Description:
The main objective of this proposed research is to *provide state DOTs a practical and cost-effective long-term fatigue crack monitoring methodology using* ***a wireless elastomeric skin sensor network****.* This research is intended to demonstrate the value-added of fatigue crack monitoring of steel bridges using wireless skin sensors over the traditional bridge inspection.

Progress this Quarter (includes meetings, work plan status, contract status, significant progress, etc.):

ISU Progress:

Task 1 (ISU): Crack sensor fabrication.

Under this task, fatigue crack sensors are to be produced with an approximate thickness of 100-200 μm to enhance the mechanical robustness under harsh environment. Acceptable ranges of capacitance is 800-1000 pF. The anticipated number of sensors is 150 to 200 for the duration of the project. Fabricated sensors are listed in Table 1.

Table 1 – produced sensors

		Capacitance	Dielectric Thickness		Resistance
Sensor	Date cast:	(pF)	(mm)	std dev	(kOhm)
61-63		Info not available			
64	5/8/2016	823	0.162	0.0058	17.8
65	5/8/2016	792	0.168	0.0075	18.3
66	5/8/2016	796	0.163	0.0067	18.0
67	5/8/2016	826	0.157	0.0085	17.5
68	5/8/2016	800	0.165	0.0085	18.2
69	5/8/2016	863	0.144	0.0094	17.4
70	5/8/2016	854	0.168	0.0071	17.2
71	5/8/2016	813	0.152	0.0034	18.2
72	5/8/2016	886	0.153	0.0053	16.9
73	5/8/2016	867	0.150	0.0071	17.4
74	5/8/2016	848	0.156	0.0101	17.7
75	6/14/2016	829	0.158	0.0048	18.2
76	6/14/2016	847	0.151	0.0091	18.2
77	6/14/2016	801	0.162	0.0053	19.7
78	6/14/2016	839	0.151	0.0080	18.8
79	6/14/2016	830	0.147	0.0067	18.9
80	6/14/2016	855	0.156	0.0076	18.3
81	6/14/2016	828	0.159	0.0076	19.3
82	6/15/2016	800	0.160	0.0071	18.9
83	6/15/2016	827	0.151	0.0080	18.5
84	6/15/2016	820	0.155	0.0053	18.6
85	6/15/2016	823	0.147	0.0033	18.2
86	6/15/2016	848	0.150	0.0047	17.4
87	6/16/2016	839	0.159	0.0039	18.6
88	6/16/2016	804	0.154	0.0050	19.8
89	6/16/2016	814	0.161	0.0046	18.8
90	6/16/2016	841	0.153	0.0067	18.3

KU Progress:

The KU team investigated the effect of mean stress or stress ratio on the crack detection performance of the SEC sensor. A CT specimen was tested under higher mean stresses and the crack growth indicator was obtained. The results show that the SEC sensor has similar performance for crack detection under higher mean stresses, provided the stress range, or ΔK is kept the same.

UA Progress:

In this quarter, the UA team developed a new way for onboard shunt calibration of the capacitive strain sensor board that they developed. Any strain sensor/gage (i.e. SEC sensor for our project) installed on the target structure requires the calibration process, because the nominal capacitance and gain value may change under uncertain field condition.

A typical way for shunt calibration is by using one additional capacitor (fixed value) connected to the SEC sensor in parallel. However, tests showed incorrect calibration when one shunt capacitor is used. The reason is that the intrinsic impedance of the lead wire for the SEC sensors significantly affects the absolute capacitance change due to the additional shunt capacitor, causing fault calibration.

The UA team addressed this issue by using two shunt capacitors, instead of one shunt capacitor. When two shunt capacitors are used, namely, one shunt capacitor is connected and then disconnected first, then the second capacitor is connected), relative capacitance difference between the two shunt capacitors can be used, rather than the absolute capacitance values. As a result, the intrinsic impedance of the lead wire does not affect the calibration process. A series of theoretical calculation and tests validated the finding. The UA team implemented this new shunt calibration approach for capacitance-based strain sensing on the developed sensor board.

Anticipated work next quarter:

ISU: The objective of the next quarter is to produce 45 additional sensors. The production of sensors will continue until KU provides results from testing, which could lead to additional optimization (Task 2). Technical support (Task 3) is being provided to KU on a continuous basis, as well as discussion and feedback (Task 4).

KU: In the next quarter, the KU team will be looking into the threshold of stress range or ΔK for crack detection using the SEC sensor. The purpose is to understand the minimum stress range beyond which the SEC can detect fatigue crack effectively.

UA: In the next quarter, the UA team will focus on performance test with small-size SEC sensors for possible improvement in sensitivity & noise performance.

Significant Results:

Part one: Fatigue crack detection with the SEC sensor

1. The KU team performs a new experimental test on SEC sensor in this quarter. The purpose of this test is to evaluate the sensor's capability of crack monitoring under higher stress ratio.

The test setup is shown in Fig. 1. The SEC sensor was attached to the back side of the compact tension (CT) specimen. A cyclic loading is applied to the specimen using a uniaxial testing machine to generate the fatigue crack. To collect the sensor's capacitance data, an off-the-shelf data acquisition board (ACAM-PCAP02) was applied. In addition, adhesive measuring tapes were attached on the front side of the CT specimen so that the length of the crack can be measured during the test.

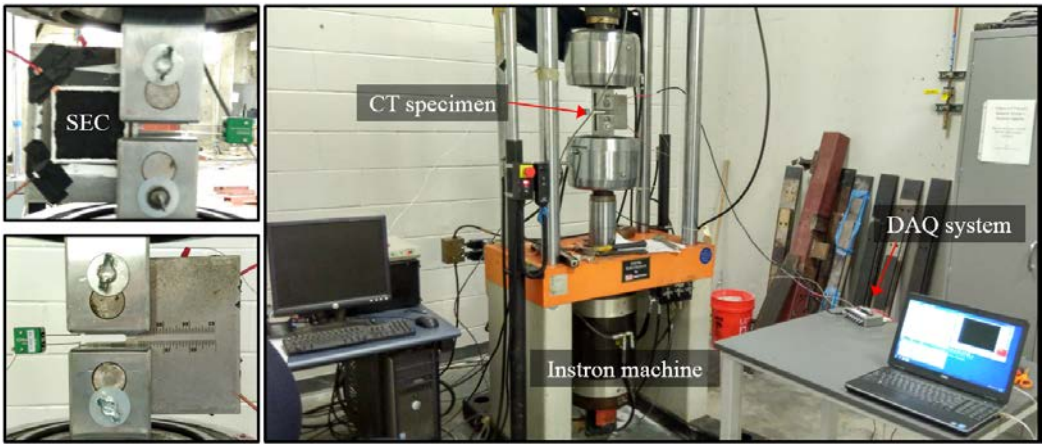

Figure 1. Test setup

The loading protocol is designed based on two criteria: 1) K (stress intensity factor) is kept around 20 ksi*in$^{1/2}$; and 2) the stress ratio R is increased to achieve loadings with higher mean values. Totally three stress ratios (R = 0.1, 0.4, and 0.6) are considered in this test. Figure 2 shows the upper and lower bounds of each loading protocol.

The fatigue crack is propagated under the high stress ratio (R = 0.6) and high loading rate (10 Hz). Once the crack reaches each additional 1/16 in, the loading rate was switched to 0.5 Hz to take three separate measurements under R = 0.1, 0.4, and 0.6, respectively. Then, the test is resumed using the previous protocol (R = 0.6, 10Hz loading rate) to continue to propagate the crack. The benefit of this data collection strategy is that three datasets can be achieved by conducting one single test.

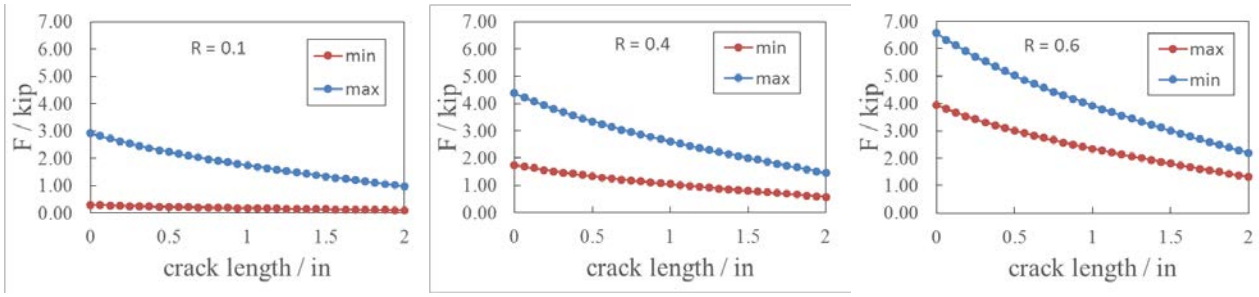

(a) (b) (c)

Figure 2 Loading protocols for different stress ratios

Figure 3 shows typical time history responses of the sensor when the crack reaches 22/16 in. in length. The capacitance measurement of the SEC sensor varies under the cyclic loading, indicating the sensor is able to capture the localized deformation caused by the cyclic loading. The peak-to-peak amplitude in Figure 3 is select as the indicator of crack growth, since such an amplitude becomes larger when the crack length is longer. Take Figure 3 as an example, the peak-to-peak amplitude of the sensor's measurement increases when the crack length is from 3/16 in to 22/16 in.

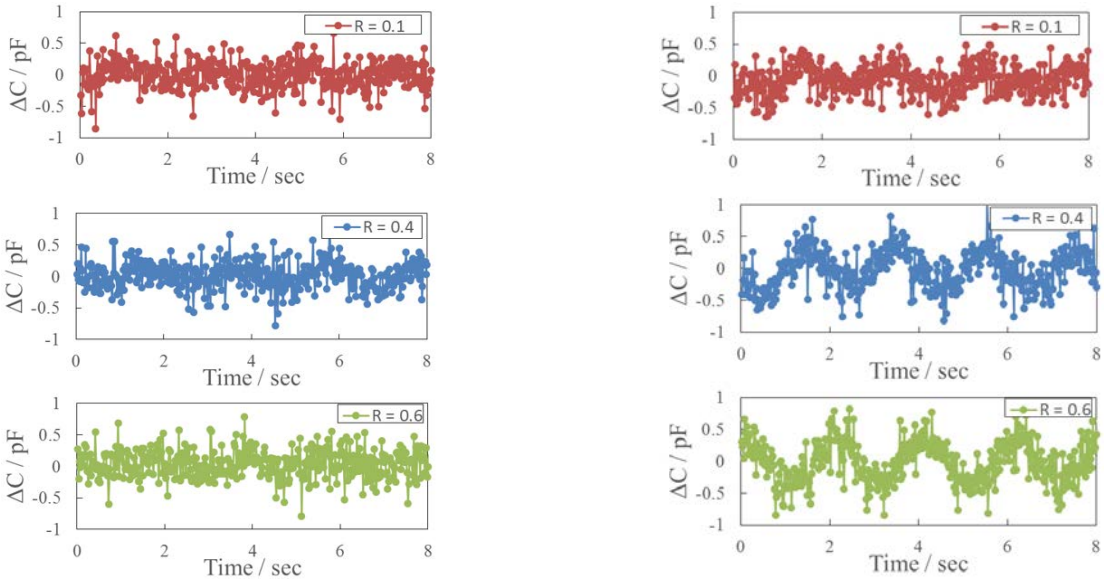

(a) (b)

Figure 3.Sensor's measurement vs. time when the crack reaches a) 3/16in; and b) 22/16 in

To extract the peak-to-peak amplitude of the sensor data more effectively, as described in the previous report, power spectral density (PSD) is adopted to capture the amplitude in frequency domain.

Figure 4 shows the PSD results under different stress ratios. For each plot, the PSD curves under different crack length are overlapped against each other. Locations of PSD peaks are labeled with crack lengths. Overall speaking, the PSD peaks go higher as the crack grows further.

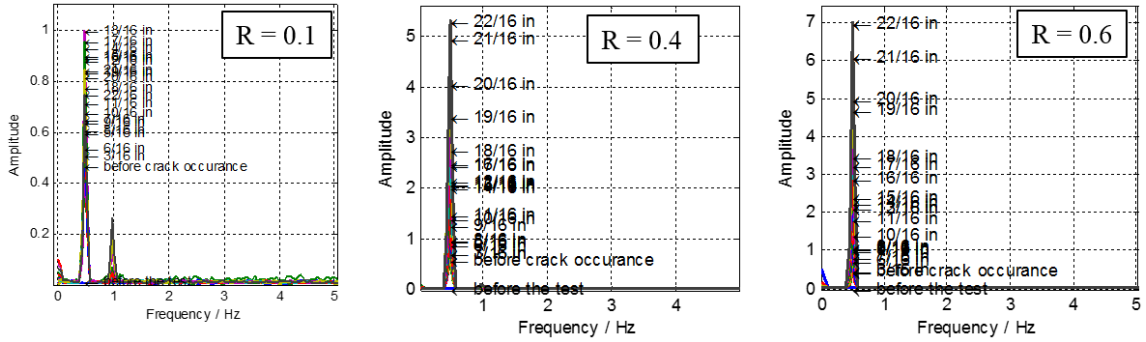

Figure 4. Power spectral densities (PSD) of the sensor's measurements

The results are further normalized by load ranges and are shown in Figure 5. The vertical axis is in logarithmic scale. The previous test result reported in last quarter is also included in this plot. The results show that the amplitude increase when the crack grows, indicating the SEC sensor can monitor the crack growth. In addition, the overall trend of the new test when R = 0.4 and 0.6 agree well with the old test results when R = 0.1. This indicates that the crack growth index based on peak-to-peak amplitude of capacitance is not affected by the mean stress or stress ratio, as long as the load range is the same. The new test result for R = 0.1 is out of the trend when the crack is large in length. This might be caused by the relaxation behavior of the sensor.

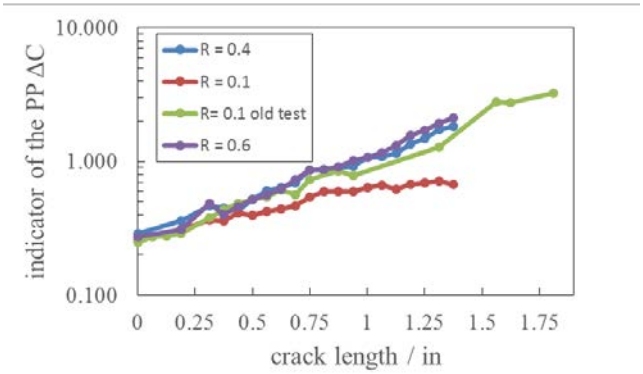

Figure 5. Normalized amplitude vs. crack length

Part two: Data acquisition sensor board development for the SEC sensor

1. Development of new onboard calibration process for the C-strain broad.

   Figure 1 illustrates the difference between the traditional shunt calibration approach and the proposed new approach.

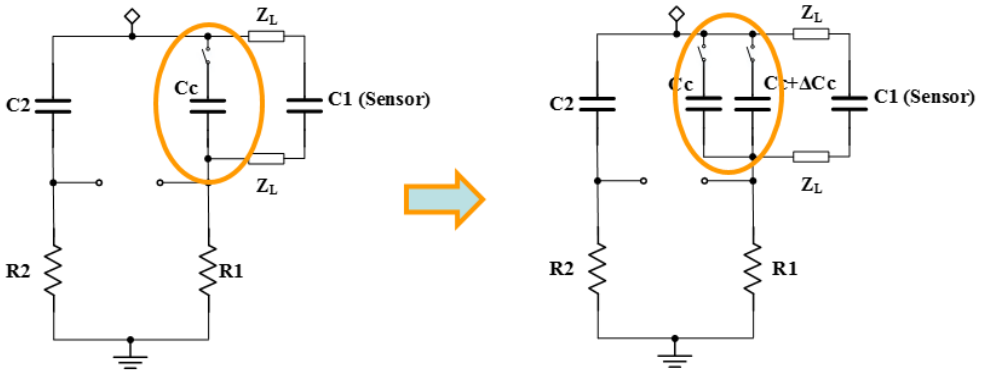

Traditional approach for shunt calibration (with single shunt capacitor, Cc above)

New shunt calibration approach using two shunt capacitors and their relative capacitance difference

Figure 1. Onboard calibration scheme for C-strain board

When only one shunt capacitor (fixed value, 4.7pF for preliminary test, see Figure 2), tests showed incorrect calibration result. As shown in Figure 2. if raw output voltage from the sensor board is calibrated using the absolute capacitance change due to additional 4.7pF, dynamic outputs (with a variable capacitor having 13pF range) do not show correct values; the maximum dynamic capacitance change (calibrated) should be 13pF, but actual dynamic change values go up to 17pF, which is incorrect. Theoretical calculation for the Wheatstone bridge showed that intrinsic impedance of the lead wires (here corresponding to C13 and C14 in below figure) affects the calibration performance.

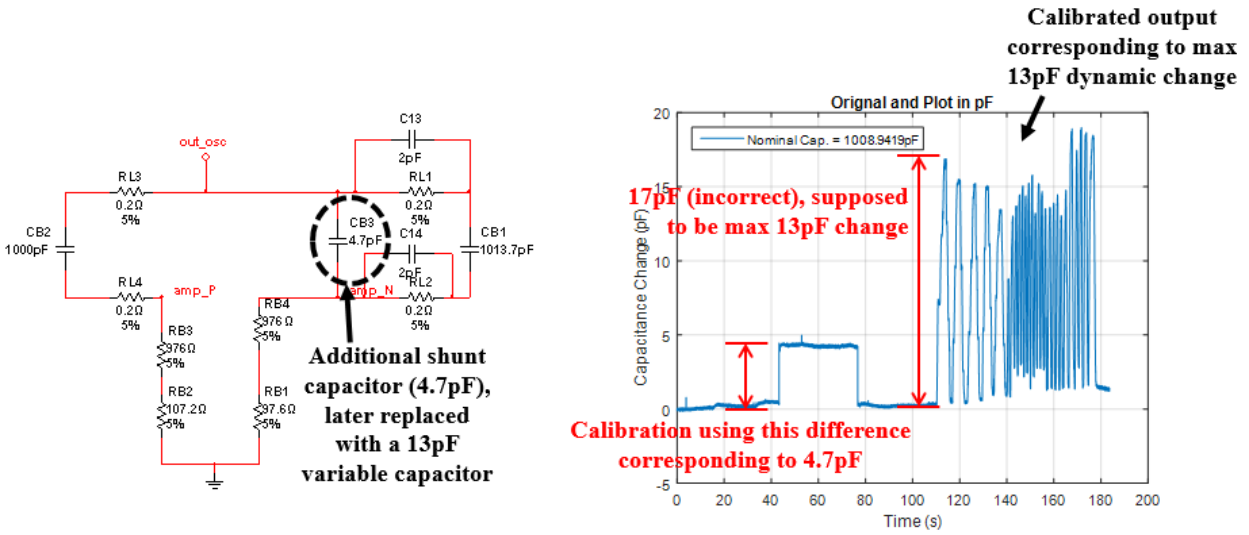

Fig 2. Onboard calibration results using traditional approach using single shunt capacitor (incorrect)

However, when two shunt capacitors and their relative capacitance difference are used for calibration, the lead wire impedances do not influence the performance.

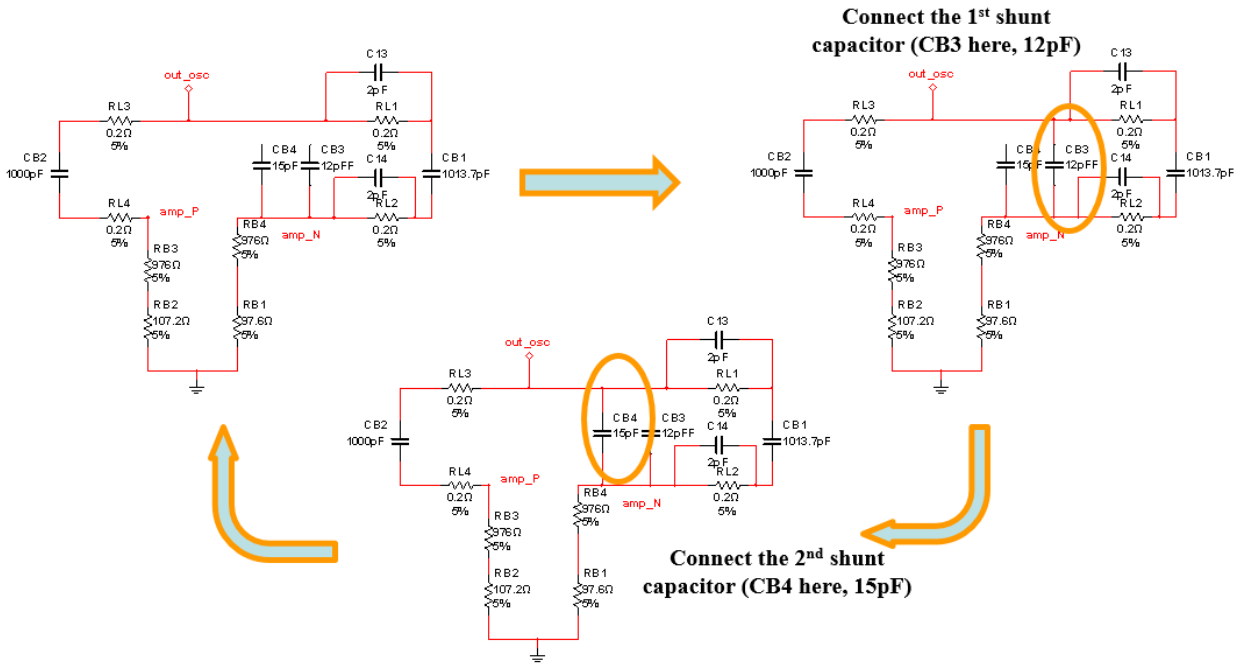

Fig 3. New onboard calibration process using two shunt capacitors and their relative difference

Figure 4 shows the results when two shunt capacitors are used. Left figure shows the raw voltage outputs from the sensor board when i) 12pF shunt capacitor is connected, ii) second 15pF shunt capacitor is connected, iii) then dynamic capacitance changes are applied using a 13pF-range variable capacitor. The right figure shows the calibrated output in pF using the relative capacitance change (in this case, it is 15-12pF = 3pF). As seen in the right size of the right figure, calibrated dynamic capacitance changes shows a max 13pF range as expected.

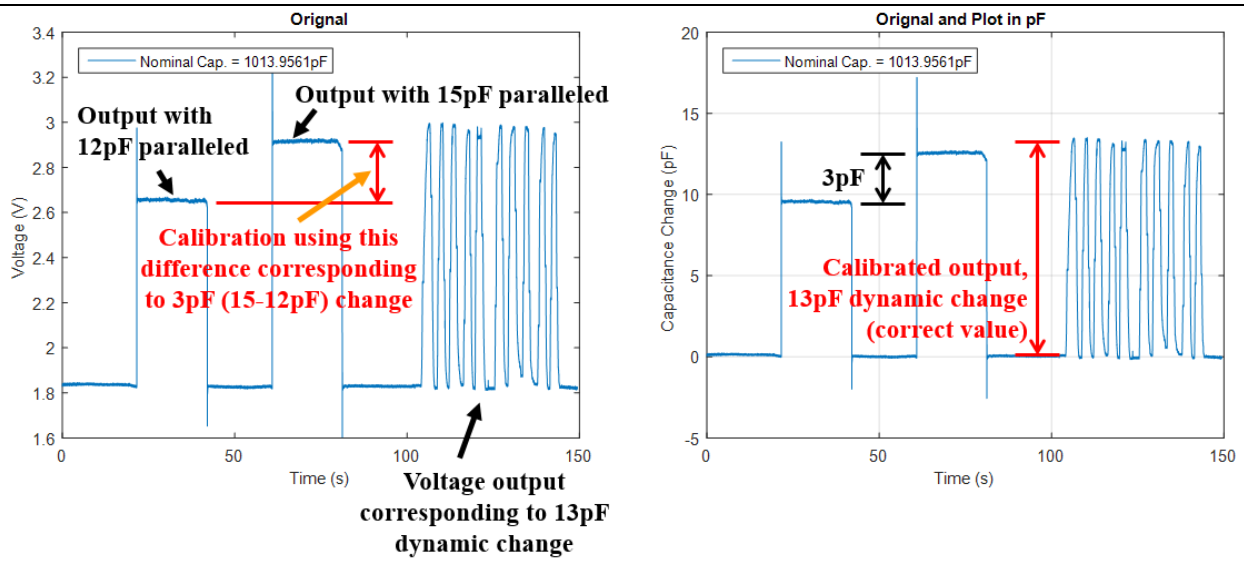

Fig 4. Shunt calibration results using the new approach with two shunt capacitors

2. Modification of the C-strain board for onboard calibration
   Figure 5 shows the block diagram and a prototype of the updated C-strain board, with the new shunt calibration approach implemented.

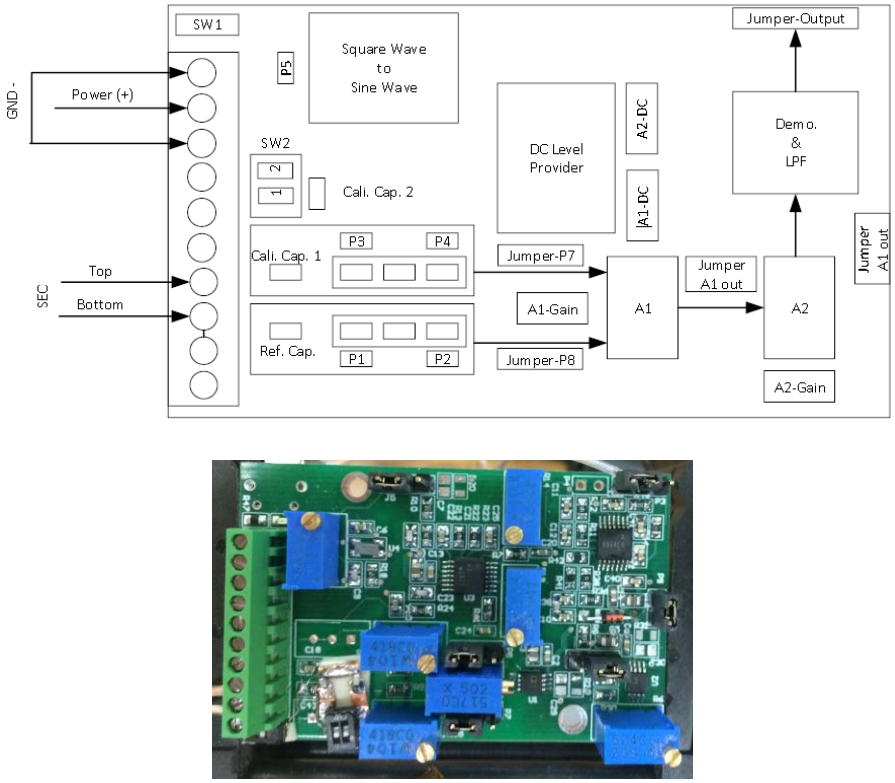

Fig 5. Block diagram (above) and new prototype of the C-strain board, incorporating onboard calibration capability.

Circumstance affecting project or budget. (Please describe any challenges encountered or anticipated that might the completion of the project within the time, scope and fiscal constraints set forth in the agreement, along with recommended solutions to those problems).

None.